Aalto University
School of Electrical
Engineering

Modular sensorless control architectures for electric machine drives

Prof. Marko Hinkkanen
IEEE Fellow

This presentation is an extended version of the plenary talk given at the *IEEE International Symposium on Sensorless Control for Electrical Drives (SLED)*, Harbin, China, 15–17 August 2025. I gratefully acknowledged my students, collaborators, and mentors.

Electric machine drives

- Example applications
  - Pumps, fans, compressors (> 75%)
  - Conveyors
  - Elevators and escalators
  - Cranes and hoists
  - Machine tools, rolling mills, etc.
  - Paper and textile industries
  - Domestic appliances
  - Electric vehicles
- External sensors avoided in industrial applications (cost, reliability, robustness. . .)
- Even if a motion sensor exists, sensorless mode often required for fault tolerance

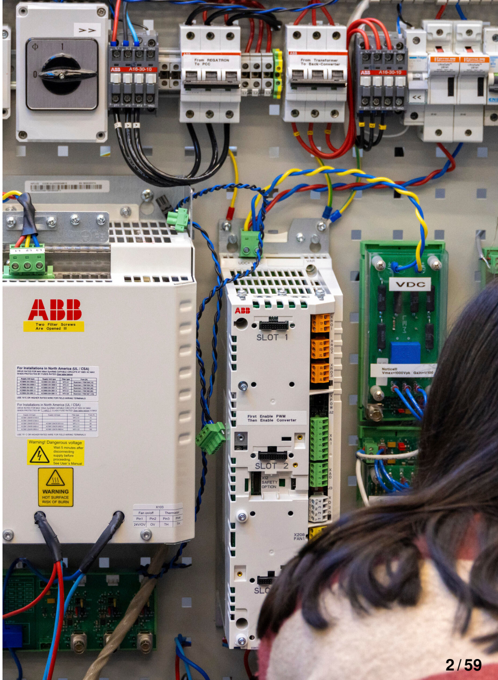

Sensorless control goals

- Produce the required speed or torque quickly and accurately at all operating points with minimum losses
- Maximize the torque for the given current limit and the DC-bus voltage
- Tolerate parameter errors
- Self-commissioning
- Monitor the drive and load condition

0. Request user input

Machine type, nameplate data

1. Identify the machine model automatically

Machine parameters, magnetic model

2. Configure the control system

Controller and observer gains, lookup tables

3. Drive the machine in an optimal manner

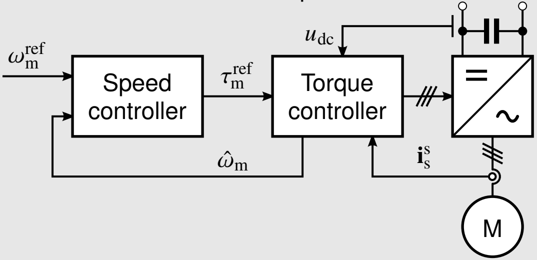

How to control all these in a unified and modular manner?

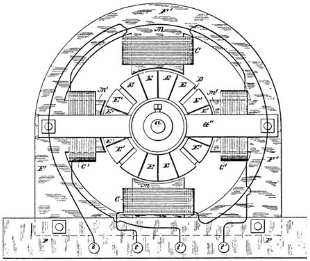

Induction machine[1]

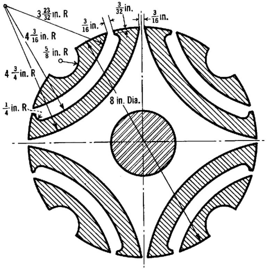

Synchronous reluctance machine (SyRM)[2]

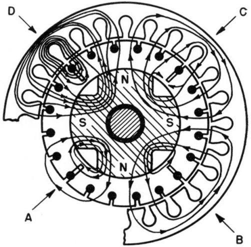

Permanent-magnet (PM) synchronous machine[3]

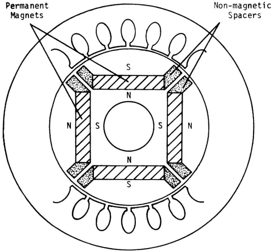

Interior PM synchronous machine[4]

[1] Tesla, ‘Electro-magnetic motor,’ *U.S. Patent 382,279*, 1888.

[2] Kostko, ‘Polyphase reaction synchronous motors,’ *J. Amer. Inst. Elect. Eng.*, 1923.

[3] Merrill, ‘Permanent-magnet excited synchronous motors,’ *AIEE Trans.*, 1955.

[4] Jahns et al., ‘Interior permanent-magnet synchronous motors for adjustable-speed drives,’ *IEEE Trans. Ind. Appl.*, 1986.

Focus and targets

Focus:

- Model-based sensorless control (signal injection left out of scope)
- Flux-vector control (simple, direct, flexible)
- Modular, decoupled observer design (applicable also to current-vector control)

Targets:

- Derive sensorless methods from fundamental machine models, allowing consistent inclusion of magnetic saturation
- Reveal analogies between different machine types
- Use same modules for different control modes (from vector to V/Hz control)

Further reading:

- Open-source Python code: *motulator*

Modular control design approach

- Same control core for multiple modes
  - High-performance vector control
  - Observer-based V/Hz control
  - Transparent current control
- Unified approach for both synchronous and induction machines
- Speed estimator as a separate module (not needed in V/Hz control)
- Shared analysis and control code
- Signal-injection module can be added[5] (but not discussed in this presentation)

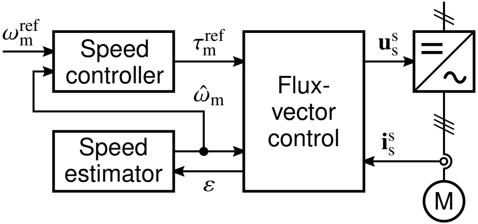

Sensorless flux-vector control

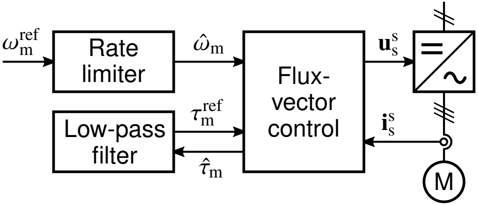

Observer-based V/Hz control

[5] Kim et al., 'PWM switching frequency signal injection sensorless method in IPMSM,' *IEEE Trans. Ind. Appl.*, 2012.

Part 1: Synchronous machines

Outline

Example: PM synchronous reluctance machine

- Reluctance machine design improved by placing PMs inside the flux barriers[6]
- PMs improve the power factor and contribute to the torque
- Low-cost ferrites can be used
- Excellent field-weakening properties
- Low risk of overvoltages due to low back-emf from PMs
- Generic model presented, but this machine type used in examples

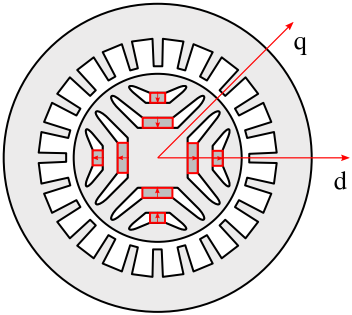

[6] Guglielmi et al., 'Position-sensorless control of permanent-magnet-assisted synchronous reluctance motor,' *IEEE Trans. Ind. Appl.*, 2004.

Space vectors and coordinate systems

- Stator current vector in stator coordinates (marked with the superscript s)

$$\mathbf{i}_\mathrm{s}^\mathrm{s} = \begin{bmatrix} i_\alpha \\ i_\beta \end{bmatrix} = \frac{2}{3}\begin{bmatrix} 1 & -1/2 & -1/2 \\ 0 & \sqrt{3}/2 & -\sqrt{3}/2 \end{bmatrix}\begin{bmatrix} i_\mathrm{a} \\ i_\mathrm{b} \\ i_\mathrm{c} \end{bmatrix}$$

- Transformation to rotor coordinates

$$\mathbf{i}_\mathrm{s} = \begin{bmatrix} i_\mathrm{d} \\ i_\mathrm{q} \end{bmatrix} = \mathrm{e}^{-\vartheta_\mathrm{m}\mathbf{J}}\mathbf{i}_\mathrm{s}^\mathrm{s}$$

- Orthogonal rotation matrix

$$\mathbf{J} = \begin{bmatrix} 0 & -1 \\ 1 & 0 \end{bmatrix}$$

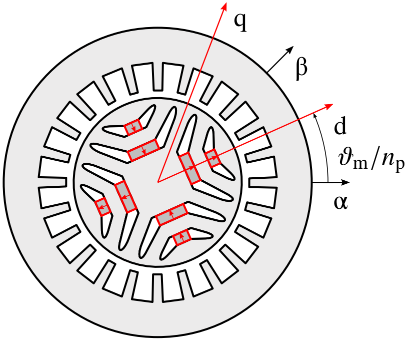

Electrical rotor speed $\omega_\mathrm{m} = \dfrac{\mathrm{d}\vartheta_\mathrm{m}}{\mathrm{d}t}$

Magnetically linear machine model in rotor coordinates

- Voltage and current equations

$$\frac{\mathrm{d}\boldsymbol{\psi}_\mathrm{s}}{\mathrm{d}t} = \mathbf{u}_\mathrm{s} - R_\mathrm{s}\mathbf{i}_\mathrm{s} - \omega_\mathrm{m}\mathbf{J}\boldsymbol{\psi}_\mathrm{s}$$
$$\mathbf{i}_\mathrm{s} = \boldsymbol{\Gamma}_\mathrm{s}(\boldsymbol{\psi}_\mathrm{s} - \boldsymbol{\psi}_\mathrm{f})$$

- Inverse inductance matrix and PM flux

$$\boldsymbol{\Gamma}_\mathrm{s} = \begin{bmatrix} 1/L_\mathrm{d} & 0 \\ 0 & 1/L_\mathrm{q} \end{bmatrix} \qquad \boldsymbol{\psi}_\mathrm{f} = \begin{bmatrix} \psi_\mathrm{f} \\ 0 \end{bmatrix}$$

- Electromagnetic torque

$$\tau_\mathrm{m} = \left[\psi_\mathrm{f} + (L_\mathrm{d} - L_\mathrm{q})i_\mathrm{d}\right] i_\mathrm{q}$$

where per-unit quantities are assumed

- How to generalize this model?

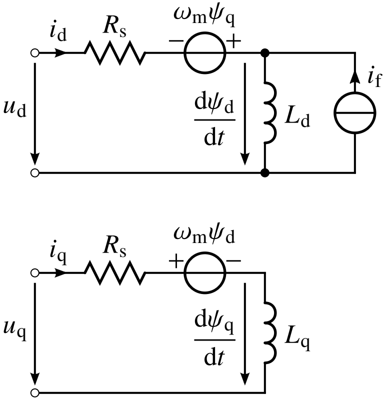

- Special cases
  - Surface magnets: $L_\mathrm{d} = L_\mathrm{q}$
  - SyRM: $\psi_\mathrm{f} = 0$

Nonlinear machine model in stator coordinates[7]

- State equations

$$\frac{\mathrm{d}\boldsymbol{\psi}_\mathrm{s}^\mathrm{s}}{\mathrm{d}t} = \mathbf{u}_\mathrm{s}^\mathrm{s} - R_\mathrm{s}\mathbf{i}_\mathrm{s}^\mathrm{s}$$
$$\frac{\mathrm{d}\vartheta_\mathrm{m}}{\mathrm{d}t} = \omega_\mathrm{m}$$

- Output equations

$$\mathbf{i}_\mathrm{s}^\mathrm{s} = \left(\frac{\partial W(\boldsymbol{\psi}_\mathrm{s}^\mathrm{s}, \vartheta_\mathrm{m})}{\partial \boldsymbol{\psi}_\mathrm{s}^\mathrm{s}}\right)^\mathsf{T} = \mathbf{g}^\mathrm{s}(\boldsymbol{\psi}_\mathrm{s}^\mathrm{s}, \vartheta_\mathrm{m})$$
$$\tau_\mathrm{m} = -\frac{\partial W(\boldsymbol{\psi}_\mathrm{s}^\mathrm{s}, \vartheta_\mathrm{m})}{\partial \vartheta_\mathrm{m}}$$

- Field energy $W(\boldsymbol{\psi}_\mathrm{s}^\mathrm{s}, \vartheta_\mathrm{m})$

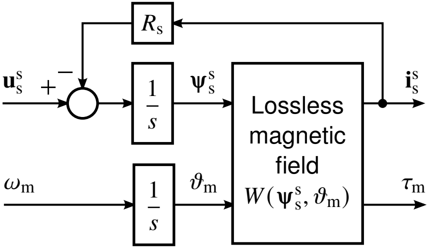

- Special case: linear magnetics

$$\mathbf{i}_\mathrm{s}^\mathrm{s} = \mathrm{e}^{\vartheta_\mathrm{m}\mathbf{J}}\boldsymbol{\Gamma}_\mathrm{s}\mathrm{e}^{-\vartheta_\mathrm{m}\mathbf{J}}\boldsymbol{\psi}_\mathrm{s}^\mathrm{s} = \boldsymbol{\Gamma}_\mathrm{s}^\mathrm{s}(\vartheta_\mathrm{m})\boldsymbol{\psi}_\mathrm{s}^\mathrm{s}$$

[7] Woodson and Melcher, *Electromechanical dynamics: Part I: Discrete systems*. 1968.

Nonlinear machine model transformed to rotor coordinates

- State equations

$$\frac{\mathrm{d}\boldsymbol{\psi}_\mathrm{s}}{\mathrm{d}t} = \mathbf{u}_\mathrm{s} - R_\mathrm{s}\mathbf{i}_\mathrm{s} - \omega_\mathrm{m}\mathbf{J}\boldsymbol{\psi}_\mathrm{s} \qquad \text{(1a)}$$

$$\frac{\mathrm{d}\vartheta_\mathrm{m}}{\mathrm{d}t} = \omega_\mathrm{m} \qquad \text{(1b)}$$

- Output equations

$$\mathbf{i}_\mathrm{s} = \left(\frac{\partial W(\boldsymbol{\psi}_\mathrm{s}, \vartheta_\mathrm{m})}{\partial \boldsymbol{\psi}_\mathrm{s}}\right)^\mathsf{T} = \mathbf{g}(\boldsymbol{\psi}_\mathrm{s}, \vartheta_\mathrm{m}) \qquad \text{(1c)}$$

$$\tau_\mathrm{m} = (\mathbf{J}\boldsymbol{\psi}_\mathrm{s})^\mathsf{T}\mathbf{i}_\mathrm{s} - \frac{\partial W(\boldsymbol{\psi}_\mathrm{s}, \vartheta_\mathrm{m})}{\partial \vartheta_\mathrm{m}} \qquad \text{(1d)}$$

- Spatial harmonic effects (gray terms) will be omitted for simplicity

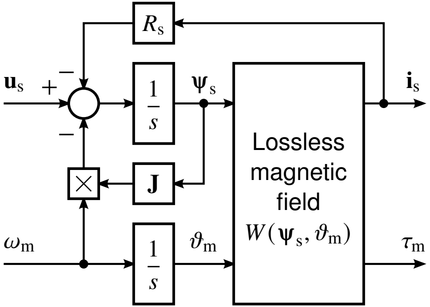

Example: Current maps $\mathbf{i}_\mathrm{s} = \mathbf{g}(\boldsymbol{\psi}_\mathrm{s})$ for a 5.6-kW PM-SyRM

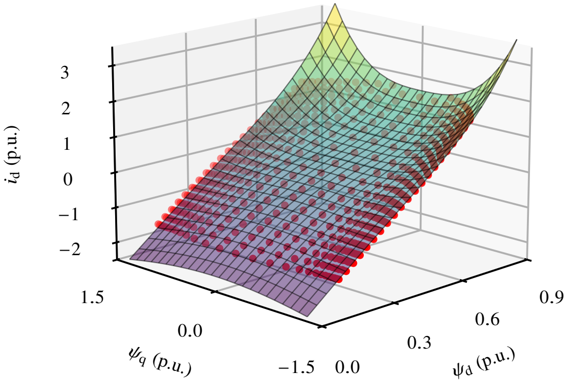

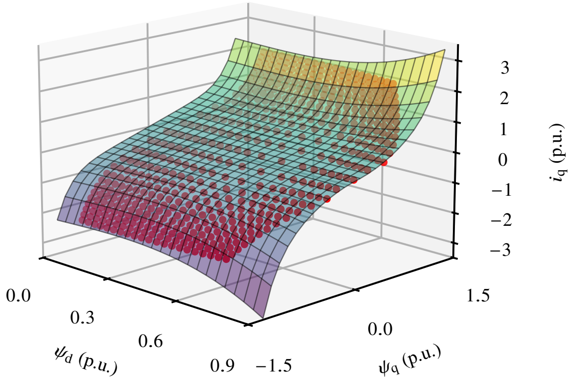

- Red markers: Measured data using the constant-speed test[8]
- Surfaces: $\mathbf{i}_\mathrm{s} = \mathbf{g}(\boldsymbol{\psi}_\mathrm{s})$ from an analytical model[9]

---

[8] Armando et al., 'Experimental identification of the magnetic model of synchronous machines,' *IEEE Trans. Ind. Appl.*, 2013.

[9] Lelli et al., 'A saturation model based on a simplified equivalent magnetic circuit for permanent magnet machines,' in *Proc. ICEM*, 2024.

Example: Flux linkage maps $\psi_s = \mathbf{f}(\mathbf{i}_s)$ for a 5.6-kW PM-SyRM

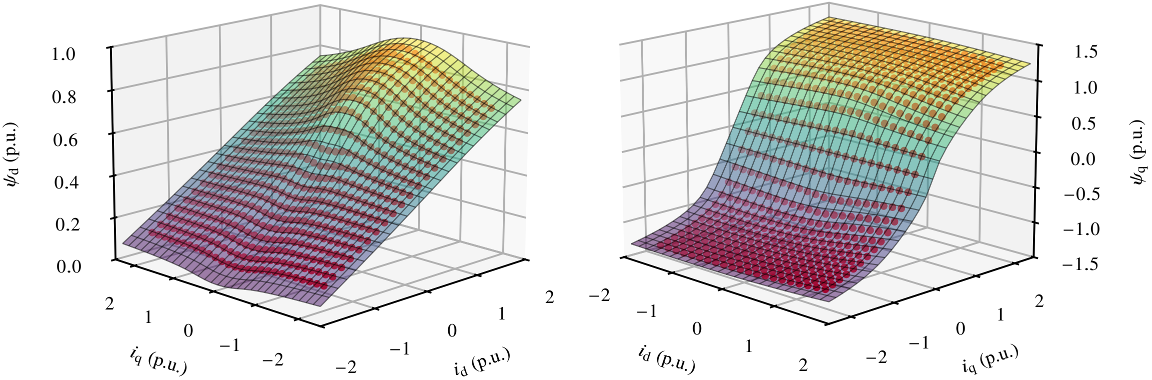

- Red markers: Same measured data as in the previous slide
- Surfaces: Numerical inverse of the analytical current map

$$\psi_s = \mathbf{f}(\mathbf{i}_s) = \mathbf{g}^{-1}(\mathbf{i}_s)$$

Flux-magnitude and torque dynamics[10]

- Model (1) yields

$$\frac{\mathrm{d}\psi_\mathrm{s}}{\mathrm{d}t} = \frac{\partial \psi_\mathrm{s}(\boldsymbol{\psi}_\mathrm{s})}{\partial \boldsymbol{\psi}_\mathrm{s}} \frac{\mathrm{d}\boldsymbol{\psi}_\mathrm{s}}{\mathrm{d}t} = \frac{\boldsymbol{\psi}_\mathrm{s}^\mathsf{T}}{\psi_\mathrm{s}}(\mathbf{u}_\mathrm{s} - R_\mathrm{s}\mathbf{i}_\mathrm{s} - \omega_\mathrm{m}\mathbf{J}\boldsymbol{\psi}_\mathrm{s}) \tag{2a}$$

$$\frac{\mathrm{d}\tau_\mathrm{m}}{\mathrm{d}t} = \frac{\partial \tau_\mathrm{m}(\boldsymbol{\psi}_\mathrm{s})}{\partial \boldsymbol{\psi}_\mathrm{s}} \frac{\mathrm{d}\boldsymbol{\psi}_\mathrm{s}}{\mathrm{d}t} = (\mathbf{J}\mathbf{i}_\mathrm{a})^\mathsf{T}(\mathbf{u}_\mathrm{s} - R_\mathrm{s}\mathbf{i}_\mathrm{s} - \omega_\mathrm{m}\mathbf{J}\boldsymbol{\psi}_\mathrm{s}) \tag{2b}$$

where $\psi_\mathrm{s} = \|\boldsymbol{\psi}_\mathrm{s}\| = \sqrt{\boldsymbol{\psi}_\mathrm{s}^\mathsf{T}\boldsymbol{\psi}_\mathrm{s}}$

- Auxiliary current

$$\mathbf{i}_\mathrm{a}(\boldsymbol{\psi}_\mathrm{s}) = -\mathbf{i}_\mathrm{s} - \mathbf{J}\boldsymbol{\Gamma}_\mathrm{s}\mathbf{J}\boldsymbol{\psi}_\mathrm{s}$$

where $\mathbf{i}_\mathrm{s} = \mathbf{g}(\boldsymbol{\psi}_\mathrm{s})$ and

$$\boldsymbol{\Gamma}_\mathrm{s}(\boldsymbol{\psi}_\mathrm{s}) = \frac{\partial \mathbf{i}_\mathrm{s}}{\partial \boldsymbol{\psi}_\mathrm{s}} \qquad (\boldsymbol{\Gamma}_\mathrm{s} = \boldsymbol{\Gamma}_\mathrm{s}^\mathsf{T})$$

- Auxiliary current is torque gradient w.r.t. flux linkage (rotated by 90°)
- Vector $\mathbf{u}_\mathrm{s} - R_\mathrm{s}\mathbf{i}_\mathrm{s} - \omega_\mathrm{m}\mathbf{J}\boldsymbol{\psi}_\mathrm{s}$ can be set via the stator voltage $\mathbf{u}_\mathrm{s}$

[10] Tiitinen et al., 'Design framework for sensorless control of synchronous machine drives,' *IEEE Trans. Ind. Electron.*, 2025.

MTPV condition[11]

- Auxiliary current $\mathbf{i}_\mathrm{a}$ allows a compact expression for the MTPV condition
- Consider flux vector $\boldsymbol{\psi}_\mathrm{s} = \mathrm{e}^{\gamma\mathbf{J}}\begin{bmatrix}\psi_\mathrm{s}\\0\end{bmatrix}$ with given magnitude ψ_s

$$\frac{\partial\tau_\mathrm{m}(\boldsymbol{\psi}_\mathrm{s})}{\partial\gamma} = \underbrace{\frac{\partial\tau_\mathrm{m}(\boldsymbol{\psi}_\mathrm{s})}{\partial\boldsymbol{\psi}_\mathrm{s}}}_{(\mathbf{J}\mathbf{i}_\mathrm{a})^\mathsf{T}} \underbrace{\frac{\partial\boldsymbol{\psi}_\mathrm{s}}{\partial\gamma}}_{\mathbf{J}\boldsymbol{\psi}_\mathrm{s}} = \mathbf{i}_\mathrm{a}^\mathsf{T}\boldsymbol{\psi}_\mathrm{s} = 0$$

- This condition is valid also for saturable machines

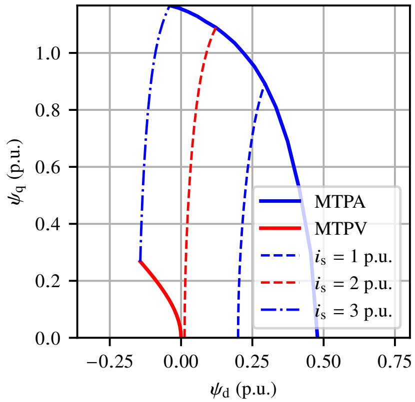

MTPA, MTPV, and constant current loci in the flux linkage plane

[11] Varatharajan et al., 'Direct flux vector control of synchronous motor drives: Accurate decoupled control with online adaptive maximum torque per ampere and maximum torque per volts evaluation,' *IEEE Trans. Ind. Electron.*, 2022.

Note: Vectors $\mathbf{i}_\mathrm{a}$ and $\boldsymbol{\psi}_\mathrm{a}$ defined in this presentation are rotated 90° compared to those in ref. 11.

MTPA condition[11]

- Consider current vector $\mathbf{i}_\mathrm{s} = \mathrm{e}^{\gamma\mathbf{J}}\left[\begin{smallmatrix} i_\mathrm{s} \\ 0 \end{smallmatrix}\right]$ with given magnitude i_s

$$\frac{\partial \tau_\mathrm{m}(\mathbf{i}_\mathrm{s})}{\partial \gamma} = \underbrace{\frac{\partial \tau_\mathrm{m}(\mathbf{i}_\mathrm{s})}{\partial \mathbf{i}_\mathrm{s}}}_{(\mathbf{J}\boldsymbol{\psi}_\mathrm{a})^\mathsf{T}} \underbrace{\frac{\partial \mathbf{i}_\mathrm{s}}{\partial \gamma}}_{\mathbf{J}\mathbf{i}_\mathrm{s}} = \boldsymbol{\psi}_\mathrm{a}^\mathsf{T}\mathbf{i}_\mathrm{s} = 0$$

- Auxiliary flux linkage

$$\boldsymbol{\psi}_\mathrm{a}(\mathbf{i}_\mathrm{s}) = \boldsymbol{\psi}_\mathrm{s} + \mathbf{J}\mathbf{L}_\mathrm{s}\mathbf{J}\mathbf{i}_\mathrm{s}$$

where $\boldsymbol{\psi}_\mathrm{s} = \mathbf{f}(\mathbf{i}_\mathrm{s})$ and

$$\mathbf{L}_\mathrm{s}(\mathbf{i}_\mathrm{s}) = \frac{\partial \boldsymbol{\psi}_\mathrm{s}}{\partial \mathbf{i}_\mathrm{s}} \qquad (\mathbf{L}_\mathrm{s} = \mathbf{L}_\mathrm{s}^\mathsf{T})$$

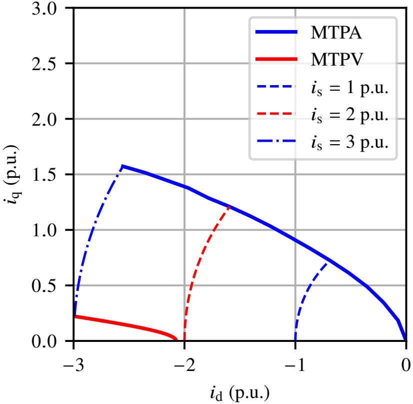

MTPA, MTPV, and constant current loci in the current plane

Outline

Optimal reference generation

- Flux and torque references simpler to generate than current references[12]
- Only 1D-lookup tables needed (5.6-kW PM-SyRM as an example)

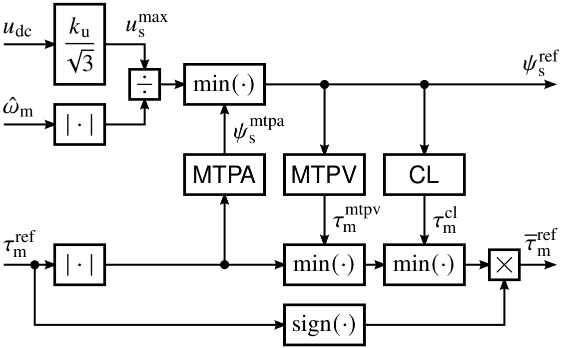

CL = current limitation

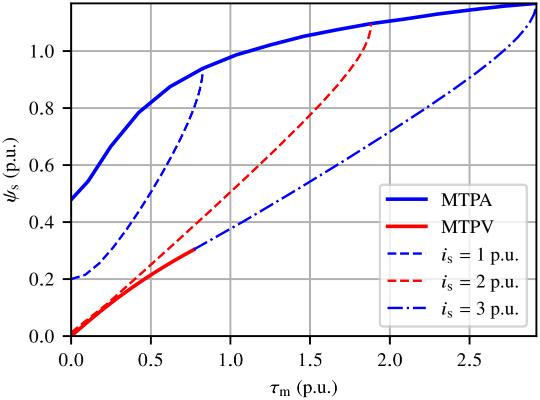

[12] Meyer and Böcker, 'Optimum control for interior permanent magnet synchronous motors (IPMSM) in constant torque and flux weakening range,' in *Proc. EPE-PEMC*, 2006.

Decoupled flux-vector control[10,13]

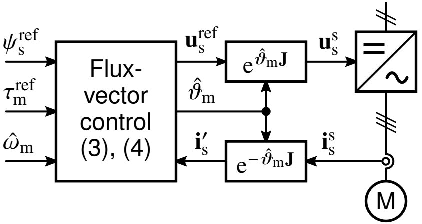

- Feedback linearization[14] of (1) yields nonlinear state feedback

$$\mathbf{u}_\mathrm{s}^\mathrm{ref} = \hat{R}_\mathrm{s}\mathbf{i}_\mathrm{s}' + \hat{\omega}_\mathrm{m}\mathbf{J}\hat{\boldsymbol{\psi}}_\mathrm{s} + \mathbf{e} \qquad \text{(3a)}$$

where the control error term is

$$\begin{aligned}\mathbf{e} = {} & k_\psi(\psi_\mathrm{s}^\mathrm{ref} - \hat{\psi}_\mathrm{s})\hat{\mathbf{i}}_\mathrm{a} \\ & + k_\tau(\tau_\mathrm{m}^\mathrm{ref} - \hat{\tau}_\mathrm{m})\mathbf{J}\hat{\boldsymbol{\psi}}_\mathrm{s}\end{aligned} \qquad \text{(3b)}$$

- Torque estimate

$$\hat{\tau}_\mathrm{m} = (\mathbf{J}\hat{\boldsymbol{\psi}}_\mathrm{s})^\mathsf{T}\mathbf{i}_\mathrm{s}' \qquad \text{(3c)}$$

- Gains giving bandwidths α_ψ and α_τ

$$k_\psi = \frac{\alpha_\psi\hat{\psi}_\mathrm{s}}{\hat{\mathbf{i}}_\mathrm{a}^\mathsf{T}\hat{\boldsymbol{\psi}}_\mathrm{s}} \qquad k_\tau = \frac{\alpha_\tau}{\hat{\mathbf{i}}_\mathrm{a}^\mathsf{T}\hat{\boldsymbol{\psi}}_\mathrm{s}} \qquad \text{(3d)}$$

where $\hat{\mathbf{i}}_\mathrm{a}^\mathsf{T}\hat{\boldsymbol{\psi}}_\mathrm{s} > 0$ always holds
- Signal $\hat{\omega}_\mathrm{m}$ can be measured, estimated or reference speed

[13] Awan et al., 'Stator-flux-oriented control of synchronous motors: A systematic design procedure,' *IEEE Trans. Ind. Appl.*, 2019.

[14] Khalil, *Nonlinear systems*, 2nd. Prentice-Hall, 1996.

State observer[15,16,17]

- Nonlinear state observer based on (1)

$$\frac{\mathrm{d}\hat{\boldsymbol{\psi}}_\mathrm{s}}{\mathrm{d}t} = \mathbf{u}_\mathrm{s}^\mathrm{ref} - \hat{R}_\mathrm{s}\mathbf{i}'_\mathrm{s} - \omega_\mathrm{c}\mathbf{J}\hat{\boldsymbol{\psi}}_\mathrm{s} + \mathbf{K}_\mathrm{o}\mathbf{e}_\mathrm{o} \quad \text{(4a)}$$

$$\frac{\mathrm{d}\hat{\vartheta}_\mathrm{m}}{\mathrm{d}t} = \hat{\omega}_\mathrm{m} + k_{\mathrm{o}\vartheta}\varepsilon = \omega_\mathrm{c} \quad \text{(4b)}$$

- Flux and rotor angle estimation errors

$$\mathbf{e}_\mathrm{o} = \hat{\mathbf{f}}(\mathbf{i}'_\mathrm{s}) - \hat{\boldsymbol{\psi}}_\mathrm{s} \quad \text{(4c)}$$

$$\varepsilon = -\frac{(\mathbf{J}\hat{\boldsymbol{\psi}}_\mathrm{a})^\mathsf{T}\mathbf{e}_\mathrm{o}}{\hat{\psi}_\mathrm{a}^2} \quad \text{(4d)}$$

- Decoupling gain[17]

$$\mathbf{K}_\mathrm{o} = (\beta_\mathrm{o}\mathbf{I} + k_\mathrm{o}\hat{\omega}_\mathrm{m}\mathbf{J})\frac{\hat{\boldsymbol{\psi}}_\mathrm{a}\hat{\boldsymbol{\psi}}_\mathrm{a}^\mathsf{T}}{\hat{\psi}_\mathrm{a}^2} \quad \text{(4e)}$$

where $\beta_\mathrm{o} > 0$ and $k_\mathrm{o} > -1$

- Formulation (3) and (4) takes magnetic saturation into account
- For linear magnetics, the flux map reduces to $\hat{\mathbf{f}}(\mathbf{i}'_\mathrm{s}) = \hat{\mathbf{L}}\mathbf{i}'_\mathrm{s} + \hat{\boldsymbol{\psi}}_\mathrm{f}$

---

15 Capecchi et al., 'Position-sensorless control of the transverse-laminated synchronous reluctance motor,' *IEEE Trans. Ind. Appl.*, 2001.

16 Piippo et al., 'Analysis of an adaptive observer for sensorless control of interior permanent magnet synchronous motors,' *IEEE Trans. Ind. Electron.*, 2008.

17 Hinkkanen et al., 'Observers for sensorless synchronous motor drives: Framework for design and analysis,' *IEEE Trans. Ind. Appl.*, 2018.

Analysis: State observer[17]

- Angle estimation error: $\tilde{\vartheta}_\mathrm{m} = \vartheta_\mathrm{m} - \hat{\vartheta}_\mathrm{m}$
- Flux estimation error in rotor coordinates:
  $\tilde{\boldsymbol{\psi}}_\mathrm{s} = \boldsymbol{\psi}_\mathrm{s} - \mathrm{e}^{-\tilde{\vartheta}_\mathrm{m}\mathbf{J}}\hat{\boldsymbol{\psi}}_\mathrm{s}$
- Linearized dynamics resulting from (1) and (4)

$$\frac{\mathrm{d}\Delta\tilde{\boldsymbol{\psi}}_\mathrm{s}}{\mathrm{d}t} = -(\omega_\mathrm{m0}\mathbf{J} + \mathbf{K}_\mathrm{o})\Delta\tilde{\boldsymbol{\psi}}_\mathrm{s} + \overbrace{\mathbf{K}_\mathrm{o}\mathbf{J}\boldsymbol{\psi}_\mathrm{a0}\Delta\tilde{\vartheta}_\mathrm{m}}^{0} \tag{5a}$$

$$\frac{\mathrm{d}\Delta\tilde{\vartheta}_\mathrm{m}}{\mathrm{d}t} = -k_{\mathrm{o}\vartheta}\Delta\tilde{\vartheta}_\mathrm{m} + \Delta\tilde{\omega}_\mathrm{m} - \frac{k_{\mathrm{o}\vartheta}(\mathbf{J}\boldsymbol{\psi}_\mathrm{a0})^\mathsf{T}}{\psi_\mathrm{a0}^2}\Delta\tilde{\boldsymbol{\psi}}_\mathrm{s} \tag{5b}$$

$$\Delta\varepsilon = \Delta\tilde{\vartheta}_\mathrm{m} - \frac{(\mathbf{J}\boldsymbol{\psi}_\mathrm{a0})^\mathsf{T}}{\psi_\mathrm{a0}^2}\Delta\tilde{\boldsymbol{\psi}}_\mathrm{s} \tag{5c}$$

where $\hat{R}_\mathrm{s} = R_\mathrm{s}$ and $\hat{\mathbf{f}} = \mathbf{f}$ are assumed

- Flux estimation error is decoupled from angle estimation error!
- Characteristic polynomial

$$s^2 + \beta_\mathrm{o}s + (1 + k_\mathrm{o})\omega_\mathrm{m0}^2$$

- Poles placed via β_o and k_o
- Angle tracking dynamics

$$\Delta\tilde{\vartheta}_\mathrm{m}(s) = \frac{\Delta\tilde{\omega}_\mathrm{m}(s)}{s + k_{\mathrm{o}\vartheta}}$$

Gain selection example

- Closed-loop poles placed in the vicinity of the open-loop poles for robustness
- Natural frequency not varied: $k_\mathrm{o} = 0$
- Damping increased

$$\beta_\mathrm{o} = \beta'_\mathrm{o} + 2\zeta_\infty|\hat{\omega}_\mathrm{m}|$$

  where β'_o defines the zero-speed pole and ζ_∞ is the damping ratio at high speeds
- Resulting poles
  - Zero speed: $s = 0$ and $s = -\beta'_\mathrm{o}$
  - High speeds: $s = -(\zeta_\infty \pm \mathrm{j}\sqrt{1-\zeta_\infty^2})|\omega_\mathrm{m0}|$
- Unstable double pole at $s = 0$ is avoided, enabling stable start of the machine

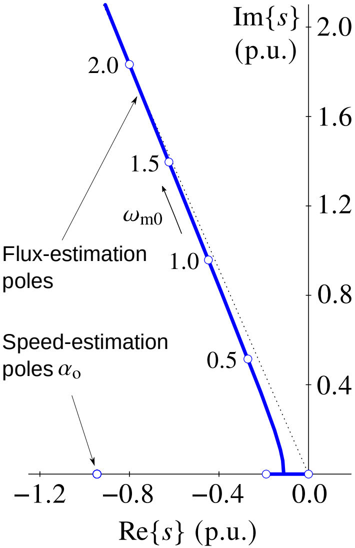

Analysis: Control law[10]

- Linearized closed-loop dynamics resulting from (2) and (3)

$$\frac{\mathrm{d}\Delta\psi_\mathrm{s}}{\mathrm{d}t} = \alpha_\psi(\Delta\psi_\mathrm{s}^\mathrm{ref} - \Delta\psi_\mathrm{s}) + \boldsymbol{\beta}_\psi^\mathsf{T}\Delta\tilde{\boldsymbol{\psi}}_\mathrm{s} \quad \text{(6a)}$$

$$\frac{\mathrm{d}\Delta\tau_\mathrm{m}}{\mathrm{d}t} = \alpha_\tau(\Delta\tau_\mathrm{m}^\mathrm{ref} - \Delta\tau_\mathrm{m}) - \mathbf{i}_\mathrm{a0}^\mathsf{T}\boldsymbol{\psi}_\mathrm{s0}\Delta\tilde{\omega}_\mathrm{m} + \boldsymbol{\beta}_\tau^\mathsf{T}\Delta\tilde{\boldsymbol{\psi}}_\mathrm{s} \quad \text{(6b)}$$

  where vectors $\boldsymbol{\beta}_\psi$ and $\boldsymbol{\beta}_\tau$ aggregate flux estimation error effects

- Term $\mathbf{i}_\mathrm{a0}^\mathsf{T}\boldsymbol{\psi}_\mathrm{s0}\Delta\tilde{\omega}_\mathrm{m}$ is specific to sensorless control

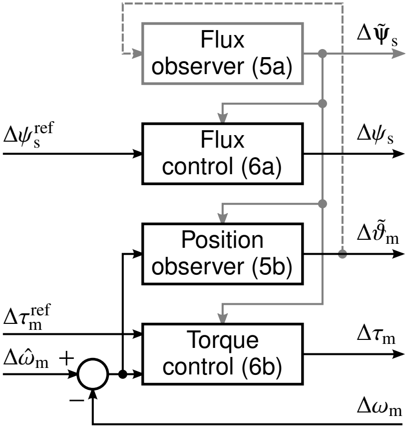

Outline

Speed estimation

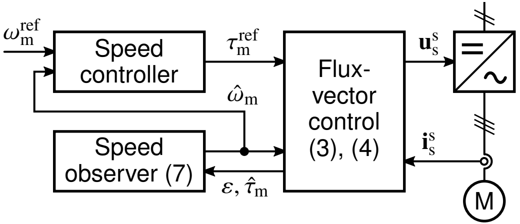

- Observer based on the mechanical system model

$$\frac{\mathrm{d}\hat{\omega}_\mathrm{m}}{\mathrm{d}t} = \frac{1}{\hat{J}}(\hat{\tau}_\mathrm{m} - \hat{\tau}_\mathrm{L}) + k_{\mathrm{o}\omega}\varepsilon \qquad \text{(7a)}$$

$$\frac{\mathrm{d}\hat{\tau}_\mathrm{L}}{\mathrm{d}t} = -k_{\mathrm{o}\tau}\varepsilon \qquad \text{(7b)}$$

- Originally used in servo drives with incremental encoders[18] and signal-injection methods[19]

- Special case: reduced-order estimator ($k_{\mathrm{o}\tau} = 0$ and $\hat{J} = \infty$)

$$\frac{\mathrm{d}\hat{\omega}_\mathrm{m}}{\mathrm{d}t} = k_{\mathrm{o}\omega}\varepsilon \qquad \text{(8)}$$

- With angle estimation (4b), this equals a typical PI mechanism[17]

[18] Lorenz and Van Patten, 'High-resolution velocity estimation for all-digital, AC servo drives,' *IEEE Trans. Ind. Appl.*, 1991.

[19] Kim et al., 'Sensorless control of interior permanent-magnet machine drives with zero-phase lag position estimation,' *IEEE Trans. Ind. Appl.*, 2003.

Analysis: Speed estimation

- Assume a mechanical system model (with $\mathrm{d}\tau_\mathrm{L}/\mathrm{d}t = 0$)

$$\frac{\mathrm{d}\omega_\mathrm{m}}{\mathrm{d}t} = \frac{1}{J}(\tau_\mathrm{m} - \tau_\mathrm{L})$$

- Linearized estimation error dynamics

$$\frac{\mathrm{d}\Delta\tilde{\omega}_\mathrm{m}}{\mathrm{d}t} = -k_{\mathrm{o}\omega}\Delta\tilde{\vartheta}_\mathrm{m} - \frac{1}{\hat{J}}\tilde{\tau}_\mathrm{L} - \frac{\tilde{J}}{\hat{J}}\frac{\mathrm{d}\Delta\omega_\mathrm{m}}{\mathrm{d}t} + \left(\frac{\boldsymbol{i}_\mathrm{s0}^\top \mathbf{J}}{\hat{J}} + \frac{k_{\mathrm{o}\omega}(\mathbf{J}\boldsymbol{\psi}_\mathrm{a0})^\top}{\psi_\mathrm{a0}^2}\right)\Delta\tilde{\boldsymbol{\psi}}_\mathrm{s} \tag{9a}$$

$$\frac{\mathrm{d}\Delta\tilde{\tau}_\mathrm{L}}{\mathrm{d}t} = k_{\mathrm{o}\tau}\Delta\tilde{\vartheta}_\mathrm{m} - \frac{k_{\mathrm{o}\tau}(\mathbf{J}\boldsymbol{\psi}_\mathrm{a0})^\top}{\psi_\mathrm{a0}^2}\Delta\tilde{\boldsymbol{\psi}}_\mathrm{s} \tag{9b}$$

- Transfer function resulting from (5b) and (9)

$$\frac{\Delta\hat{\omega}_\mathrm{m}(s)}{\Delta\omega_\mathrm{m}(s)} = \frac{(J/\hat{J})s^3 + (J/\hat{J})k_{\mathrm{o}\vartheta}s^2 + k_{\mathrm{o}\omega}s + k_{\mathrm{o}\tau}/\hat{J}}{s^3 + k_{\mathrm{o}\vartheta}s^2 + k_{\mathrm{o}\omega}s + k_{\mathrm{o}\tau}/\hat{J}}$$

- If $\hat{J} = J$, speed estimation has no lag
- Observer is robust to the inertia estimate and damping[18]
- Critically damped poles (transfer function below assumes $\hat{J} = J$)

$$k_{\mathrm{o}\vartheta} = 3\alpha_\mathrm{o} \quad k_{\mathrm{o}\omega} = 3\alpha_\mathrm{o}^2 \quad k_{\mathrm{o}\tau} = \alpha_\mathrm{o}^3 \hat{J} \quad \Rightarrow \quad \frac{\Delta\hat{\omega}_\mathrm{m}(s)}{\Delta\omega_\mathrm{m}(s)} = \frac{(s+\alpha_\mathrm{o})^3}{(s+\alpha_\mathrm{o})^3} = 1$$

- Special case: critically damped reduced-order estimator

$$k_{\mathrm{o}\vartheta} = 2\alpha_\mathrm{o} \quad k_{\mathrm{o}\omega} = \alpha_\mathrm{o}^2 \quad k_{\mathrm{o}\tau} = 0 \quad \hat{J} = \infty \quad \Rightarrow \quad \frac{\Delta\hat{\omega}_\mathrm{m}(s)}{\Delta\omega_\mathrm{m}(s)} = \frac{\alpha_\mathrm{o}^2}{(s+\alpha_\mathrm{o})^2}$$

- Inertia estimate avoided, but lag limits achievable speed-control bandwidth[10]

Analysis: Closing the loop with speed control

- Consider PI speed control and speed observer (7)
- Loop transfer function

$$L(s) = \frac{k_p s + k_i}{s} \frac{\alpha_\tau}{s + \alpha_\tau} \frac{1}{Js}$$

- Sufficient stability condition $k_i/k_p < \alpha_\tau$ easy to fulfill
- Reduced-order estimator (8) is simpler but limits speed-control bandwidth[4]

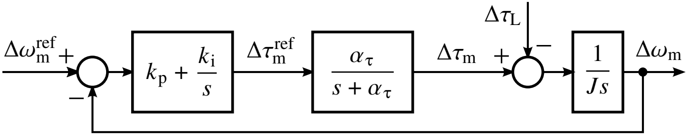

Linearized model with the speed observer (7), assuming $\hat{J} = J$

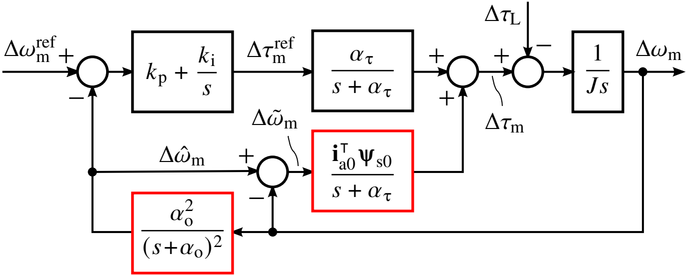

Linearized model with the reduced-order speed estimator (8)

Simulation example: Accurate parameters

- 5.6-kW PM-SyRM model (1) uses the measured map $\mathbf{i}_\mathrm{s} = \mathbf{g}(\boldsymbol{\psi}_\mathrm{s})$
- Acceleration from 0 to 2 p.u. speed, 70% load torque step at $t = 0.8$ s
- Accurately parametrized sensorless flux-vector control (3) and (4): $\hat{\mathbf{g}}(\hat{\boldsymbol{\psi}}_\mathrm{s}) = \mathbf{g}(\hat{\boldsymbol{\psi}}_\mathrm{s})$, $\hat{\mathbf{f}}(\mathbf{i}_\mathrm{s}') = \mathbf{f}(\mathbf{i}_\mathrm{s}')$, $\hat{R}_\mathrm{s} = R_\mathrm{s}$
- Speed observer (7) with critically damped poles and accurate inertia estimate $\hat{J} = J$
- Current limit $i_\mathrm{s}^\mathrm{max} = 2$ p.u.
- Current reference $\mathbf{i}_\mathrm{s}^\mathrm{ref}$ is generated and shown, but not needed in control
- 2DOF PI speed controller

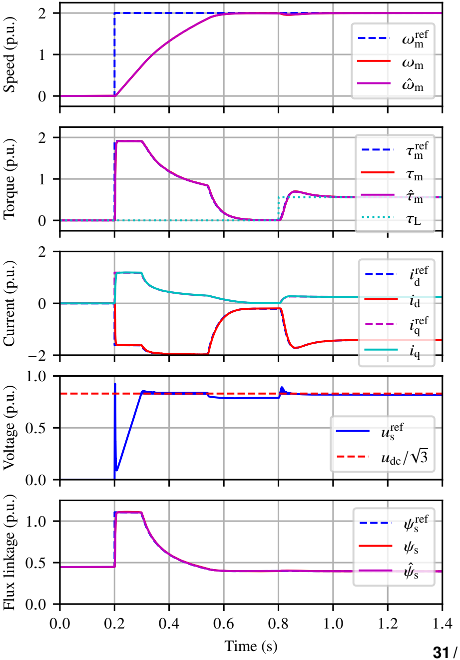

Simulation example: Parameter errors

- Control system uses estimated maps $\hat{\mathbf{g}}(\hat{\boldsymbol{\psi}}_\mathrm{s})$ and $\hat{\mathbf{f}}(\mathbf{i}'_\mathrm{s})$ from the analytical model
- Stator resistance estimate $\hat{R}_\mathrm{s} = 0.8R_\mathrm{s}$
- Speed observer with $\hat{J} = 100J$!
- Note also that flux-vector control has no integral action, but it is inherently provided by the speed observer

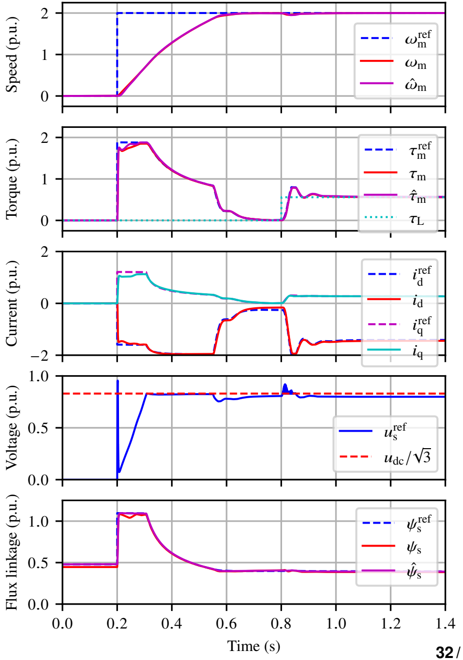

Outline

Observer-based V/Hz control[10]

- Torque reference is obtained simply by low-pass filtering the estimate

$$\frac{\mathrm{d}\tau_\mathrm{m}^\mathrm{ref}}{\mathrm{d}t} = \alpha_\mathrm{f}(\hat{\tau}_\mathrm{m} - \tau_\mathrm{m}^\mathrm{ref}) \qquad (10)$$

- Speed estimate $\hat{\omega}_\mathrm{m}$ for flux-vector control is replaced with (rate-limited) speed reference $\omega_\mathrm{m}^\mathrm{ref}$
- Neither speed controller nor speed estimator needed

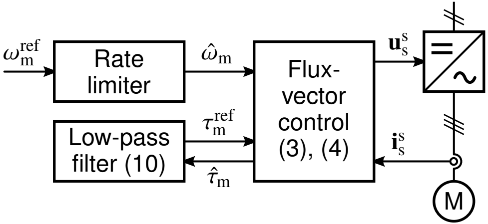

- Constant value $\psi_\mathrm{s}^\mathrm{ref}$ may be used for simplicity (leading to higher losses)
- Saturation effects are typically omitted in V/Hz control
- Works for all machine types

Concept: Passivity

- Mechanical impedance depends on the electromagnetics and control[20]

$$Z_\mathrm{m}(s) = -\frac{\Delta\tau_\mathrm{m}(s)}{\Delta\omega_\mathrm{m}(s)}$$

- Transfer function $Z_\mathrm{m}(s)$ passive if[14]

$$\mathrm{Re}\{Z_\mathrm{m}(\mathrm{j}\omega)\} \geq 0 \quad \text{for all } \omega$$

- Mechanical systems (admittances)

$$Y_\mathrm{m}(s) = \frac{\Delta\omega_\mathrm{m}(s)}{\Delta\tau_\mathrm{m}(s)} \quad \text{e.g.} \quad Y_\mathrm{m}(s) = \frac{1}{Js}$$

are typically passive

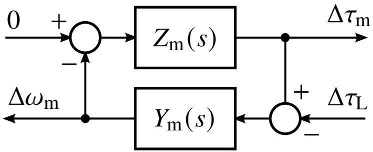

- Negative feedback interconnection of passive systems is passive
- Passivity is sufficient (not necessary) condition for stability
- With passive $Z_\mathrm{m}(s)$, the closed-loop system is stable for any (unknown) passive mechanical system

[20] Hartikainen et al., 'Identification of mechanical impedance of an electric machine drive for drivetrain design,' in *Proc. IEEE IEMDC*, 2023.

Analysis: Observer-based V/Hz control

- Mechanical impedance[10]

$$Z_{\mathrm{m}}(s) = \frac{s + \alpha_{\mathrm{f}}}{s + \alpha_{\tau} + \alpha_{\mathrm{f}}} \frac{\mathbf{i}_{\mathrm{a0}}^{\mathsf{T}} \boldsymbol{\psi}_{\mathrm{s0}}}{s}$$

- With positive α_{τ} and α_{f}, the mechanical impedance is passive in the whole feasible operating region
- Observer-based V/Hz control is locally stable for any passive mechanics

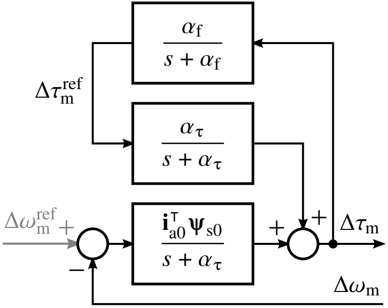

Flux linkage maps $\boldsymbol{\psi}_{\mathrm{s}} = \mathbf{f}(\mathbf{i}_{\mathrm{s}})$ for a 6.7-kW SyRM

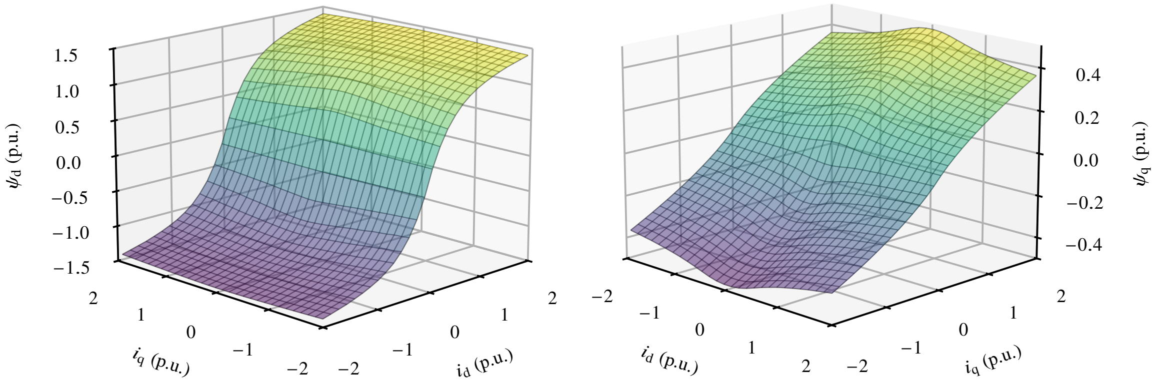

- Analytical current map $\mathbf{i}_{\mathrm{s}} = \mathbf{g}(\boldsymbol{\psi}_{\mathrm{s}})$ was fitted to the measured data
- Flux maps shown here are the numerical inverse $\boldsymbol{\psi}_{\mathrm{s}} = \mathbf{f}(\mathbf{i}_{\mathrm{s}}) = \mathbf{g}^{-1}(\mathbf{i}_{\mathrm{s}})$

Simulation example: Speed reversals and quadratic load

- 6.7-kW SyRM model (1) characterized using the map $\mathbf{i}_\mathrm{s} = \mathbf{g}(\boldsymbol{\psi}_\mathrm{s})$ described above
- Quadratic load torque $\tau_\mathrm{L} = k_\mathrm{L}\omega_\mathrm{m}^2$
- Observer-based V/Hz control (3), (4), (10) uses constant inductances $\hat{L}_\mathrm{d}$ and $\hat{L}_\mathrm{q}$
- Flux reference is constant $\psi_\mathrm{s}^\mathrm{ref} = 1$ p.u.

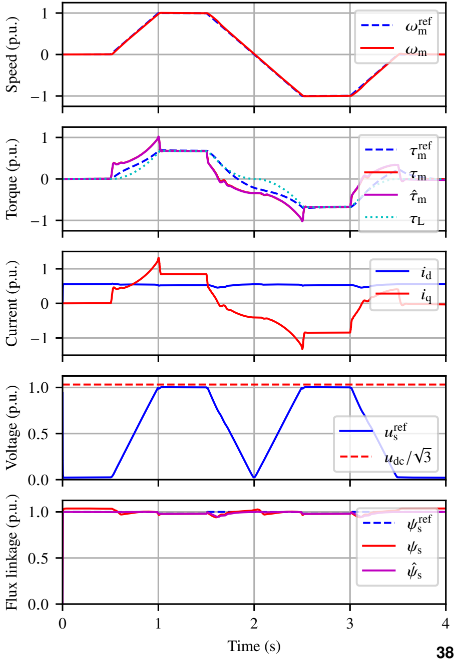

Part 2: Induction machines

Outline

Induction machine modelling

Decoupled sensorless flux-vector control

Speed estimation

Observer-based V/Hz control

Γ model with main-flux saturation[21]

- State equations in general coordinates rotating at ω_c

$$\frac{d\boldsymbol{\psi}_s}{dt} = \mathbf{u}_s - R_s\mathbf{i}_s - \omega_c\mathbf{J}\boldsymbol{\psi}_s \tag{11a}$$

$$\frac{d\boldsymbol{\psi}_r}{dt} = -R_r\mathbf{i}_r - (\omega_c - \omega_m)\mathbf{J}\boldsymbol{\psi}_r \tag{11b}$$

- Currents

$$\mathbf{i}_s = \frac{\boldsymbol{\psi}_s - \gamma\boldsymbol{\psi}_r}{\gamma L_\ell} \tag{11c}$$

$$\mathbf{i}_r = \frac{\boldsymbol{\psi}_r - \boldsymbol{\psi}_s}{L_\ell} \tag{11d}$$

- Magnetic coupling factor

$$\gamma = \frac{L_s}{L_s + L_\ell} \tag{11e}$$

- Electromagnetic torque

$$\tau_m = (\mathbf{J}\boldsymbol{\psi}_s)^\top \mathbf{i}_s = \frac{(\mathbf{J}\boldsymbol{\psi}_r)^\top \boldsymbol{\psi}_s}{L_\ell} \tag{11f}$$

- Main-flux saturation $L_s = L_s(\psi_s)$ can be directly modeled, giving $\gamma = \gamma(\psi_s)$

[21] Slemon, 'Modelling of induction machines for electric drives,' *IEEE Trans. Ind. Appl.*, 1989.

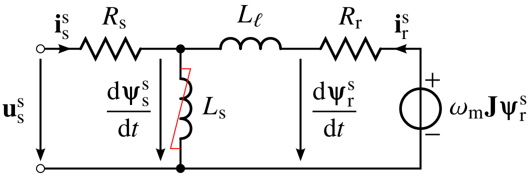

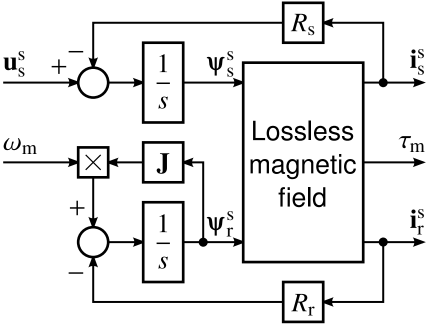

- Example saturation function[22]

$$L_s(\psi_s) = \frac{L_{su}}{1 + (\beta\psi_s)^S} \qquad L_{su} = \text{unsaturated inductance}$$

- Leakage inductance saturation and deep-bar effect could be included[23]

[22] Qu et al., 'Loss-minimizing flux level control of induction motor drives,' *IEEE Trans. Ind. Appl.*, 2012.

[23] Mölsä et al., 'A dynamic model for saturated induction machines with closed rotor slots and deep bars,' *IEEE Trans. Energy Convers.*, 2020.

Flux-magnitude and torque dynamics[24]

- Model (11) yields

$$\frac{\mathrm{d}\psi_\mathrm{s}}{\mathrm{d}t} = \frac{\partial\psi_\mathrm{s}(\boldsymbol{\psi}_\mathrm{s})}{\partial\boldsymbol{\psi}_\mathrm{s}}\frac{\mathrm{d}\boldsymbol{\psi}_\mathrm{s}}{\mathrm{d}t} = \frac{\boldsymbol{\psi}_\mathrm{s}^\mathsf{T}}{\psi_\mathrm{s}}(\mathbf{u}_\mathrm{s} - R_\mathrm{s}\mathbf{i}_\mathrm{s} - \omega_\mathrm{m}\mathbf{J}\boldsymbol{\psi}_\mathrm{s}) \tag{12a}$$

$$\begin{aligned}\frac{\mathrm{d}\tau_\mathrm{m}}{\mathrm{d}t} &= \frac{\partial\tau_\mathrm{m}(\boldsymbol{\psi}_\mathrm{s},\boldsymbol{\psi}_\mathrm{r})}{\partial\boldsymbol{\psi}_\mathrm{s}}\frac{\mathrm{d}\boldsymbol{\psi}_\mathrm{s}}{\mathrm{d}t} + \frac{\partial\tau_\mathrm{m}(\boldsymbol{\psi}_\mathrm{s},\boldsymbol{\psi}_\mathrm{r})}{\partial\boldsymbol{\psi}_\mathrm{r}}\frac{\mathrm{d}\boldsymbol{\psi}_\mathrm{r}}{\mathrm{d}t} \\ &= \frac{(\mathbf{J}\boldsymbol{\psi}_\mathrm{r})^\mathsf{T}}{L_\ell}[\mathbf{u}_\mathrm{s} - R_\mathrm{s}\mathbf{i}_\mathrm{s} - (\omega_\mathrm{m}+\omega_\mathrm{r})\mathbf{J}\boldsymbol{\psi}_\mathrm{s}]\end{aligned} \tag{12b}$$

- Slip angular frequency

$$\omega_\mathrm{r} = \frac{\omega_\mathrm{rb}(\mathbf{J}\boldsymbol{\psi}_\mathrm{r})^\mathsf{T}\boldsymbol{\psi}_\mathrm{s}}{\boldsymbol{\psi}_\mathrm{r}^\mathsf{T}\boldsymbol{\psi}_\mathrm{s}} \qquad \omega_\mathrm{rb} = \frac{R_\mathrm{r}}{L_\ell} \tag{12c}$$

[24] Tiitinen et al., ‘Sensorless flux-vector control framework: An extension for induction machines,’ *IEEE Trans. Ind. Electron.*, 2025.

Inverse-Γ model for control purposes, with main-flux saturation

- Model (11) yields

$$\frac{\mathrm{d}\boldsymbol{\psi}_\mathrm{s}}{\mathrm{d}t} = \mathbf{u}_\mathrm{s} - R_\mathrm{s}\mathbf{i}_\mathrm{s} - \omega_\mathrm{c}\mathbf{J}\boldsymbol{\psi}_\mathrm{s} \tag{13a}$$

$$L_\sigma\frac{\mathrm{d}\mathbf{i}_\mathrm{s}}{\mathrm{d}t} = \mathbf{u}_\mathrm{s} - (R_\sigma\mathbf{I} + \omega_\mathrm{c}L_\sigma\mathbf{J})\mathbf{i}_\mathrm{s} + (\alpha\mathbf{I} - \omega_\mathrm{m}\mathbf{J})\,\boldsymbol{\psi}_\mathrm{R} - \boldsymbol{\epsilon} \tag{13b}$$

$$\boldsymbol{\psi}_\mathrm{R} = \boldsymbol{\psi}_\mathrm{s} - L_\sigma\mathbf{i}_\mathrm{s} = \gamma\boldsymbol{\psi}_\mathrm{r} \tag{13c}$$

- Saturation induces a transient voltage (omitted in the following)

$$\boldsymbol{\epsilon} = \frac{1}{\gamma(\psi_\mathrm{s})}\frac{\partial\gamma(\psi_\mathrm{s})}{\partial\psi_\mathrm{s}}\frac{\boldsymbol{\psi}_\mathrm{s}\boldsymbol{\psi}_\mathrm{s}^\mathsf{T}}{\psi_\mathrm{s}}(\mathbf{u}_\mathrm{s} - R_\mathrm{s}\mathbf{i}_\mathrm{s})$$

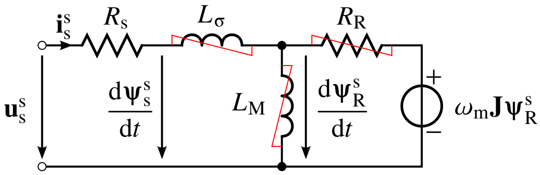

- Parameters are nonlinear in flux magnitude due to $\gamma = \gamma(\psi_\mathrm{s})$

$$L_\sigma = \gamma L_\ell \qquad L_\mathrm{M} = \gamma L_\mathrm{s} \qquad R_\mathrm{R} = \gamma^2 R_\mathrm{r}$$

$$\alpha = R_\mathrm{R}/L_\mathrm{M} \qquad R_\sigma = R_\mathrm{s} + R_\mathrm{R}$$

Outline

Decoupled flux-vector control[19]

- Control law based on (12)

$$\mathbf{u}_\mathrm{s}^\mathrm{ref} = \hat{R}_\mathrm{s}\mathbf{i}_\mathrm{s} + (\hat{\omega}_\mathrm{m}+\hat{\omega}_\mathrm{r})\mathbf{J}\hat{\boldsymbol{\psi}}_\mathrm{s} + \mathbf{e} \quad \text{(14a)}$$

- Decoupling control error term

$$\mathbf{e} = k_\psi(\psi_\mathrm{s}^\mathrm{ref} - \hat{\psi}_\mathrm{s})\hat{\boldsymbol{\psi}}_\mathrm{R} + k_\tau(\tau_\mathrm{m}^\mathrm{ref} - \hat{\tau}_\mathrm{m})\mathbf{J}\hat{\boldsymbol{\psi}}_\mathrm{s} \quad \text{(14b)}$$

- Torque and slip estimates

$$\hat{\tau}_\mathrm{m} = (\mathbf{J}\hat{\boldsymbol{\psi}}_\mathrm{s})^\mathsf{T}\mathbf{i}_\mathrm{s} \quad \text{(14c)}$$

$$\hat{\omega}_\mathrm{r} = \frac{\hat{\omega}_\mathrm{rb}(\mathbf{J}\hat{\boldsymbol{\psi}}_\mathrm{R})^\mathsf{T}\hat{\boldsymbol{\psi}}_\mathrm{s}}{\hat{\boldsymbol{\psi}}_\mathrm{R}^\mathsf{T}\hat{\boldsymbol{\psi}}_\mathrm{s}} \quad \text{(14d)}$$

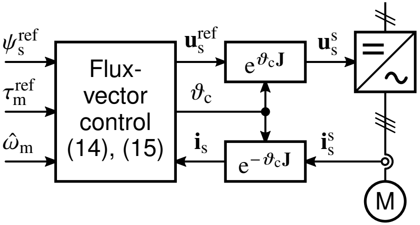

- Gains giving bandwidths α_ψ and α_τ

$$k_\psi = \frac{\alpha_\psi\hat{\psi}_\mathrm{s}}{\hat{\boldsymbol{\psi}}_\mathrm{R}^\mathsf{T}\hat{\boldsymbol{\psi}}_\mathrm{s}} \qquad k_\tau = \frac{\alpha_\tau L_\sigma}{\hat{\boldsymbol{\psi}}_\mathrm{R}^\mathsf{T}\hat{\boldsymbol{\psi}}_\mathrm{s}} \quad \text{(14e)}$$

  where $\hat{\boldsymbol{\psi}}_\mathrm{R}^\mathsf{T}\hat{\boldsymbol{\psi}}_\mathrm{s} > 0$ always holds
- Signal $\hat{\omega}_\mathrm{m}$ can be measured, estimated or reference speed

Reduced-order flux observer[25]

- State observer based on (13)

$$\frac{\mathrm{d}\hat{\boldsymbol{\psi}}_\mathrm{s}}{\mathrm{d}t} = \mathbf{u}_\mathrm{s}^\mathrm{ref} - \hat{R}_\mathrm{s}\mathbf{i}_\mathrm{s} - \omega_\mathrm{c}\mathbf{J}\hat{\boldsymbol{\psi}}_\mathrm{s} + \mathbf{K}_\mathrm{o}\mathbf{e}_\mathrm{o} \quad \text{(15a)}$$

$$\hat{\boldsymbol{\psi}}_\mathrm{R} = \hat{\boldsymbol{\psi}}_\mathrm{s} - \hat{L}_\sigma \mathbf{i}_\mathrm{s} \quad \text{(15b)}$$

- Voltage estimation error

$$\mathbf{e}_\mathrm{o} = \hat{L}_\sigma \frac{\mathrm{d}\mathbf{i}_\mathrm{s}}{\mathrm{d}t} - \mathbf{u}_\mathrm{s}^\mathrm{ref} + \left(\hat{R}_\sigma\mathbf{I} + \omega_\mathrm{c}\hat{L}_\sigma\mathbf{J}\right)\mathbf{i}_\mathrm{s} - (\hat{\alpha}\mathbf{I} - \hat{\omega}_\mathrm{m}\mathbf{J})\,\hat{\boldsymbol{\psi}}_\mathrm{R} \quad \text{(15c)}$$

- Decoupling gain

$$\mathbf{K}_\mathrm{o} = \frac{\beta_\mathrm{o}(\hat{\alpha}\mathbf{I} + \hat{\omega}_\mathrm{m}\mathbf{J})}{\hat{\alpha}^2 + \hat{\omega}_\mathrm{m}^2}\frac{\hat{\boldsymbol{\psi}}_\mathrm{R}\hat{\boldsymbol{\psi}}_\mathrm{R}^\mathsf{T}}{\hat{\psi}_\mathrm{R}^2} \quad \text{(15d)}$$

- $\beta_\mathrm{o} > 0$ defines the attenuation
- ω_c can be arbitrary (e.g. $\omega_\mathrm{c} = 0$), but synchronous coordinates preferred for discretization

$$\frac{\mathrm{d}\vartheta_\mathrm{c}}{\mathrm{d}t} = \omega_\mathrm{c} = \hat{\omega}_\mathrm{m} + \hat{\omega}_\mathrm{r} \quad \text{(15e)}$$

[25] Hinkkanen et al., ‘Reduced-order flux observers with stator-resistance adaptation for speed-sensorless induction motor drives,’ *IEEE Trans. Power Electron.*, 2010.

Analysis: Flux observer[25]

- Assume accurate parameter estimates
- Linearized estimation error $\tilde{\boldsymbol{\psi}}_\mathrm{s} = \boldsymbol{\psi}_\mathrm{s} - \hat{\boldsymbol{\psi}}_\mathrm{s}$ dynamics from (13) and (15)

$$\frac{\mathrm{d}\Delta\tilde{\boldsymbol{\psi}}_\mathrm{s}}{\mathrm{d}t} = -\left[\omega_\mathrm{s0}\mathbf{J} + \mathbf{K}_\mathrm{o}(\alpha\mathbf{I} - \omega_\mathrm{m0}\mathbf{J})\right]\Delta\tilde{\boldsymbol{\psi}}_\mathrm{s} + \underbrace{\mathbf{K}_\mathrm{o}\mathbf{J}\boldsymbol{\psi}_\mathrm{R0}\Delta\tilde{\omega}_\mathrm{m}}_{0} \tag{16a}$$

$$\Delta\mathbf{e}_\mathrm{o} = -\mathbf{J}\boldsymbol{\psi}_\mathrm{R0}\Delta\tilde{\omega}_\mathrm{m} + (\alpha\mathbf{I} - \omega_\mathrm{m0}\mathbf{J})\Delta\tilde{\boldsymbol{\psi}}_\mathrm{s} \tag{16b}$$

- Flux estimation error is decoupled from the speed estimation error!
- Resulting characteristic polynomial: $s^2 + \beta_\mathrm{o}s + \omega_\mathrm{s0}^2$
- Attenuation factor can be selected as (see slide 24)

$$\beta_\mathrm{o} = \beta_\mathrm{o}' + 2\zeta_\infty|\hat{\omega}_\mathrm{m}|$$

- β_o' defines the zero-speed pole and ζ_∞ is the high-speed damping ratio

Analysis: Control law[24]

- Linearized closed-loop dynamics resulting from (12) and (14)

$$\frac{\mathrm{d}\Delta\psi_\mathrm{s}}{\mathrm{d}t} = \alpha_\psi(\Delta\psi_\mathrm{s}^\mathrm{ref} - \Delta\psi_\mathrm{s}) + \boldsymbol{\beta}_\psi^\mathsf{T}\Delta\tilde{\boldsymbol{\psi}}_\mathrm{s} \quad \text{(17a)}$$

$$\frac{\mathrm{d}\Delta\tau_\mathrm{m}}{\mathrm{d}t} = \alpha_\tau(\Delta\tau_\mathrm{m}^\mathrm{ref} - \Delta\tau_\mathrm{m}) - \frac{\boldsymbol{\psi}_\mathrm{R0}^\mathsf{T}\boldsymbol{\psi}_\mathrm{s0}}{L_\sigma}\Delta\tilde{\omega}_\mathrm{m} + \boldsymbol{\beta}_\tau^\mathsf{T}\Delta\tilde{\boldsymbol{\psi}}_\mathrm{s} \quad \text{(17b)}$$

  where vectors $\boldsymbol{\beta}_\psi$ and $\boldsymbol{\beta}_\tau$ aggregate flux estimation error effects
- Term $\boldsymbol{\psi}_\mathrm{R0}^\mathsf{T}\boldsymbol{\psi}_\mathrm{s0}\Delta\tilde{\omega}_\mathrm{m}/L_\sigma$ is specific to sensorless control

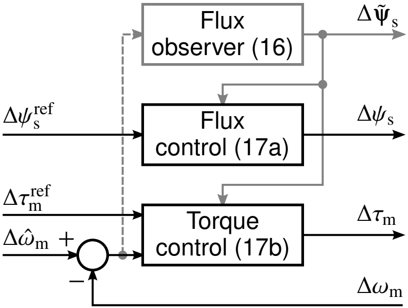

Outline

Speed estimation

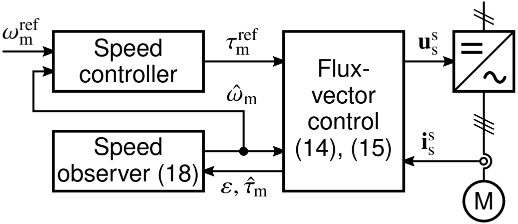

- Speed estimation error signal

$$\varepsilon = -\frac{(\mathbf{J}\hat{\boldsymbol{\psi}}_\mathrm{R})^\mathsf{T}\mathbf{e}_\mathrm{o}}{\hat{\psi}_\mathrm{R}^2}$$

- Model-based speed observer

$$\frac{\mathrm{d}\hat{\omega}_\mathrm{m}}{\mathrm{d}t} = \frac{1}{\hat{J}}(\hat{\tau}_\mathrm{m} - \hat{\tau}_\mathrm{L}) + k_{\mathrm{o}\omega}\varepsilon \qquad \text{(18a)}$$

$$\frac{\mathrm{d}\hat{\tau}_\mathrm{L}}{\mathrm{d}t} = -k_{\mathrm{o}\tau}\varepsilon \qquad \text{(18b)}$$

- Special case: reduced-order estimator ($k_{\mathrm{o}\tau} = 0$ and $\hat{J} = \infty$)

$$\frac{\mathrm{d}\hat{\omega}_\mathrm{m}}{\mathrm{d}t} = k_{\mathrm{o}\omega}\varepsilon$$

- Corresponds to slip-relation-based estimation with 1st-order LPF[25]

Analysis: Speed estimation

- Flux-estimation error omitted (appears only as an external disturbance)
- Linearized estimation error dynamics

$$\frac{\mathrm{d}\Delta\tilde{\omega}_\mathrm{m}}{\mathrm{d}t} = -k_{\mathrm{o}\omega}\Delta\tilde{\omega}_\mathrm{m} - \frac{1}{\hat{J}}\Delta\tilde{\tau}_\mathrm{L} - \frac{\tilde{J}}{\hat{J}}\frac{\mathrm{d}\Delta\omega_\mathrm{m}}{\mathrm{d}t} + \frac{1}{\hat{J}}\Delta\tilde{\tau}_\mathrm{m}$$

$$\frac{\mathrm{d}\Delta\tilde{\tau}_\mathrm{L}}{\mathrm{d}t} = k_{\mathrm{o}\tau}\Delta\tilde{\omega}_\mathrm{m}$$

- Resulting transfer function

$$\frac{\Delta\hat{\omega}_\mathrm{m}(s)}{\Delta\omega_\mathrm{m}(s)} = \frac{(J/\hat{J})s^2 + k_{\mathrm{o}\omega}s + k_{\mathrm{o}\tau}/\hat{J}}{s^2 + k_{\mathrm{o}\omega}s + k_{\mathrm{o}\tau}/\hat{J}}$$

- Critically damped poles: $k_{\mathrm{o}\omega} = 2\alpha_\mathrm{o}$ and $k_{\mathrm{o}\tau} = \alpha_\mathrm{o}^2\hat{J}$

$$\frac{\Delta\hat{\omega}_\mathrm{m}(s)}{\Delta\omega_\mathrm{m}(s)} = \frac{(s+\alpha_\mathrm{o})^2}{(s+\alpha_\mathrm{o})^2} = 1$$

  assuming $\hat{J} = J$
- Reduced-order estimator: $k_{\mathrm{o}\omega} = \alpha_\mathrm{o}$, $k_{\mathrm{o}\tau} = 0$, and $\hat{J} = \infty$

$$\frac{\Delta\hat{\omega}_\mathrm{m}(s)}{\Delta\omega_\mathrm{m}(s)} = \frac{\alpha_\mathrm{o}}{s+\alpha_\mathrm{o}}$$

Simulation example: Accurate parameters

- 2.2-kW induction machine model (11) with main-flux saturation
- Acceleration from 0 to 2 p.u. speed, 50% load torque step at $t = 0.8$ s
- Accurately parametrized sensorless flux-vector control (14) and (15)
- Speed observer (18) with critically damped poles and accurate inertia estimate $\hat{J} = J$
- Current limit $i_s^{max} = 1.5$ p.u.
- 2DOF PI speed controller

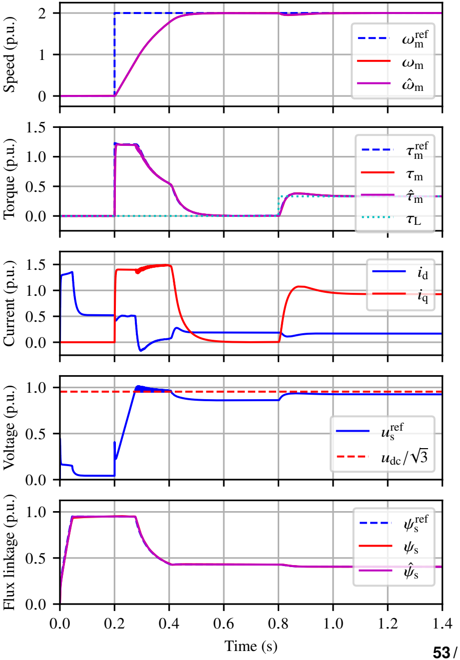

Simulation example: Parameter errors

- Control system uses constant $\hat{L}_{\mathrm{M}}$, $\hat{L}_{\sigma}$, and $\hat{R}_{\mathrm{R}}$ values
- Stator resistance estimate $\hat{R}_{\mathrm{s}} = 0.8R_{\mathrm{s}}$
- Speed observer with $\hat{J} = 100J$
- Note that oscillations appear mostly in currents, while estimated torque and stator flux are well controlled

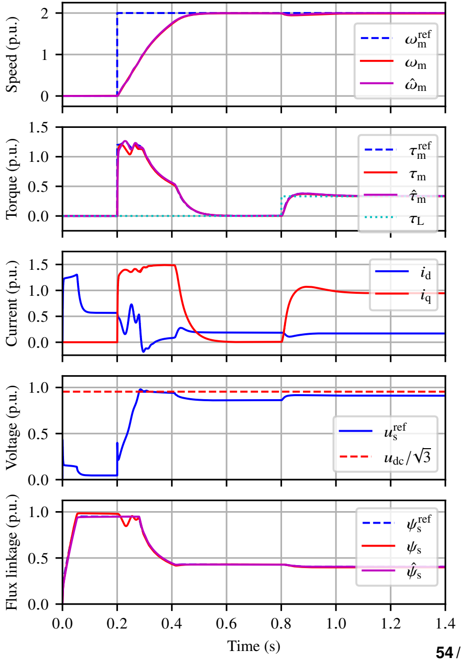

Outline

Observer-based V/Hz control

- Same architecture and analysis as for synchronous machines
- Speed estimate $\hat{\omega}_\mathrm{m}$ for flux-vector control is replaced with (rate-limited) speed reference $\omega_\mathrm{m}^\mathrm{ref}$
- Neither speed controller nor speed estimator needed
- Locally stable for any passive mechanics

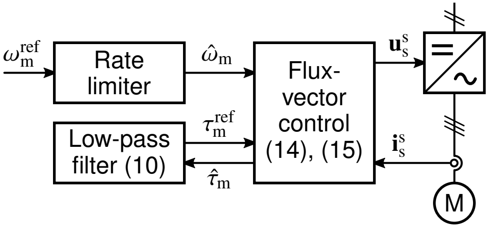

Simulation example: Observer-based V/Hz control

- 2.2-kW induction machine model (11) with main-flux saturation
- Control system uses constant parameters
- Acceleration from 0 to 1 p.u. speed, 100% load torque step at $t = 0.8$ s
- Observer acts as a model-based stabilizer and compensator (RI and slip)
- Less trial-and-error tuning needed

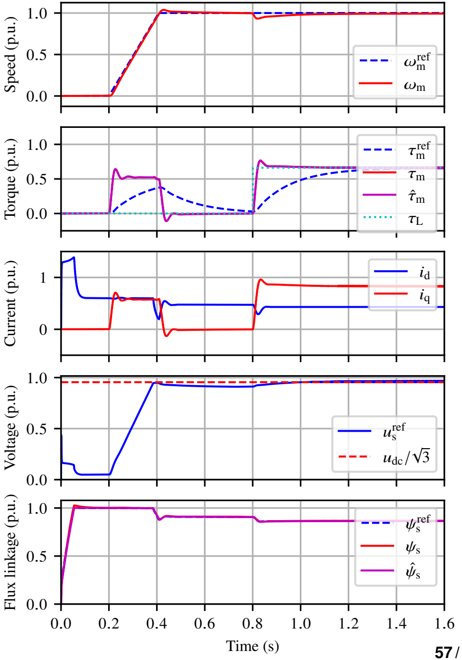

Simulation example: Open-loop V/Hz control

- Choosing $\hat{R}_\mathrm{s} = 0$ $\hat{R}_\mathrm{R} = 0$, $\hat{L}_\sigma = 0$, and $\hat{L}_\mathrm{M} = \infty$, observer-based V/Hz control falls back to open-loop V/Hz control
- If the parameters are even roughly known, the observer-based V/Hz control improves the control performance

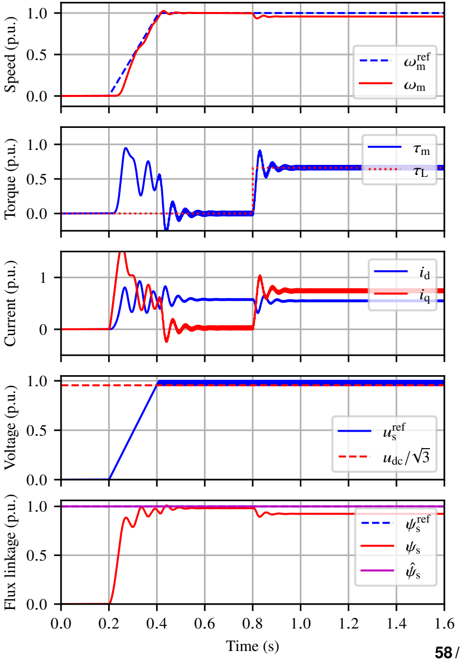

Conclusions

- Decoupled control and observer design $\Rightarrow$ modularity and simpler analysis
- Auxiliary current and flux allow consistent inclusion of saturation in control
- Reference generator, observer, and control rely on the same magnetic model
- Mechanical-model-based speed observer allows to avoid lag
- Same control structures for both synchronous and induction machines